

Heterogeneous plasmonic trimers for enhanced nonlinear optical absorption

 Seyfollah Toroghi, Chatdanai Lumdee, and Pieter G. Kik^{a),b)}

CREOL, The College of Optics and Photonics, University of Central Florida, 4000 Central Florida Blvd, Orlando, Florida 32816, USA

(Received 5 February 2015; accepted 26 February 2015; published online 10 March 2015)

A dramatic enhancement of the thermally induced nonlinear optical response in compositionally heterogeneous plasmonic trimers is reported. It is demonstrated numerically that the nonlinear absorption performance of silver nanoparticle dimers under pulsed illumination can be enhanced by more than two orders of magnitude through the addition of only 0.1 vol. % of gold in the dimer gap. The nonlinear absorption performance of the resulting Ag-Au-Ag trimer exceeds the peak performance of isolated gold nanoparticles by a factor 40. This dramatic effect is enabled by cascaded plasmon resonance, resulting in extreme field concentration in the central nanoparticle of the trimer. The observed localized heat-generation, large optical response, and a predicted response time below 1 ns make these structures promising candidates for use in nonlinear optical limiting and optical switching. © 2015 AIP Publishing LLC. [<http://dx.doi.org/10.1063/1.4914454>]

Nanoscale heat generation in metallic nanoparticle clusters under optical irradiation has received enormous attention due to the ability of plasmonic nanostructures to introduce large and extremely localized thermal gradients in a wide variety of environments. Pulsed laser excitation of metallic nanostructures produces an abrupt temperature rise inside the nanostructures, giving rise to several photothermal, and optoacoustic phenomena that can be used in bubble formation,^{1–3} selective cell targeting,^{4,5} catalytic reactions,^{6,7} optoacoustic imaging,⁸ nano-welding,^{9,10} and thermally induced optical modulation and limiting.^{11–13} In the case of the latter applications, plasmon-enhanced light absorption induces a large temperature change which causes a large modification of the dielectric function, resulting in thermally induced nonlinear absorption and scattering. To optimize these processes in plasmonic structures, one must balance the thermo-optic coefficients of all materials involved, the magnitude of the heat generation, and its spatial distribution throughout the nanostructure.

Several different approaches have been used to control heat generation in plasmonic nanostructures, including geometry optimization^{14,15} and engineered inter-particle coupling.^{16–18} Recently, we demonstrated that heterogeneous plasmonic trimer structures composed of a gold nanoparticle between two silver nanoparticles can produce a heat dissipation densities that exceed that of isolated gold nanoparticles by two orders of magnitude.¹⁹ In the present study, we numerically investigate the thermally induced nonlinear optical response of such plasmonic nanostructures using combined full-field three-dimensional electromagnetic and transient thermal calculations. We demonstrate that these structures can strongly enhance the attainable temperature change and the resulting nonlinear optical response compared to that of individual particles by leveraging the cascaded field enhancement effect. It is shown that these effects

occur on a sub-nanosecond time scale, suggesting the possibility of fast nonlinear optical switching and modulation.

To evaluate the thermo-optic response of plasmonic nonlinear absorbers, we used a combination of three-dimensional frequency domain finite integration electromagnetic simulations²⁰ and time domain finite integration thermal simulations.²¹ We initially consider three representative nanostructures: an isolated 10 nm diameter gold nanosphere, a dimer composed of two 80 nm diameter silver nanospheres, and a heterogeneous trimer structure composed of a 10 nm diameter gold nanosphere located between two 80 nm diameter silver nanospheres, all assumed to be embedded in water ($n = 1.33$). The edge-to-edge spacing between adjacent nanoparticles is set to 5 nm. Literature data were used for the dielectric functions of silver²² and gold.²³

Figure 1(a) shows the calculated absorption cross-section spectra of the three different structures determined from the simulated electric field distributions. The structures are illuminated by light propagating along the z-direction with the electric field amplitude E_0 polarized along the x-axis, corresponding to polarization along the dimer and

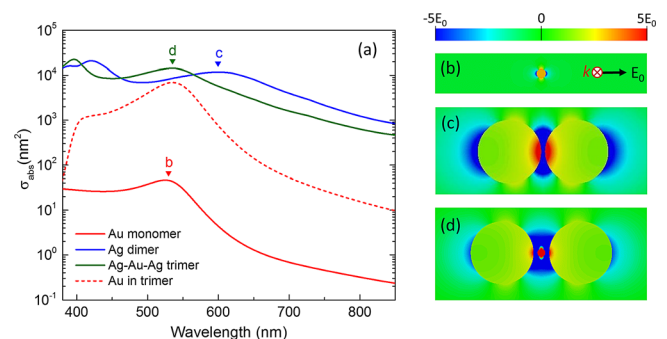


FIG. 1. (a) Absorption cross section spectra for a 10 nm diameter gold monomer (red solid line), a dimer composed of 80 nm diameter silver particles with gap of 5 nm (blue line) and a heterogeneous trimer composed of a 10 nm diameter gold nanoparticle between two 80 nm diameter silver nanospheres (green line). The dashed red line represents the fractional absorption cross-section $\sigma_{abs,Au}$ of the gold nanoparticle in the trimer structure. Electric field distribution for (b) the gold monomer, (c) the silver dimer, and (d) the heterogeneous trimer, illuminated at the wavelengths indicated in (a).

^{a)}Also at: Physics Department, University of Central Florida, 4000 Central Florida Blvd, Orlando, Florida 32816, USA

^{b)}Author to whom correspondence should be addressed. Electronic mail: kik@creol.ucf.edu

trimer axes, respectively. The absorption cross-section of the gold particle (Fig. 1(a), red line) shows a single absorption peak at 530 nm. Figure 1(b) shows a snapshot of the x-component of the simulated electric field distribution for the Au monomer at the peak wavelength in the plane normal to the light propagation direction. The field distribution is indicative of the well-known dipolar plasmon resonance mode, resulting in an electric field enhancement factor of 1.9 and consequently large optical dissipation. The absorption cross-section spectrum of the silver dimer (Fig. 1(a), blue line) shows two peaks located at 420 nm and 600 nm, respectively. The electric field distribution corresponding to the absorption peak at 600 nm is shown in Fig. 1(c), revealing a plasmon resonance with the fields on each nanoparticle having a partly dipolar character and significant field concentration near the gap. The absorption peak at 420 nm is due to the excitation of a similar hybridized plasmon resonance mode with a mixed dipolar and multipolar character. The absorption cross-section of the Ag-Au-Ag trimer structure (Fig. 1(a), green line) shows peaks located at 400 nm and 535 nm, respectively. The field distribution corresponding to the latter peak is shown in Fig. 1(d), revealing a largely dipolar field distribution on each of the three nanoparticles, oscillating approximately in-phase, i.e., the internal electric field in adjacent particles has identical sign. At this excitation frequency, the field enhancement in the Au particle is 25, a remarkably large value compared to the single particle field enhancement factor of 1.9. This is the combined result of field concentration in the dimer gap and a multiplicative cascaded plasmon resonance, in which a high-polarizability resonator excites a smaller resonator without significant loss in quality factor.²⁴ The large field enhancement achieved in this case leads to a large power dissipation in the gold particle, which is described by the gold related fractional absorption cross-section $\sigma_{\text{abs,Au}}$ (dashed red line in Fig. 1(a)) given by the ratio of the power absorbed in the Au nanoparticle and the irradiance. The maximum absorption cross-section of the gold particle inside the trimer structure is seen to be enhanced by two orders of magnitude compared to that of the gold monomer, suggesting that a large thermo-optic response and large thermal nonlinear optical absorption may be achieved in this structure.

In order to evaluate the thermally induced nonlinear optical response of the plasmonic structures discussed above, we consider pulsed excitation at frequencies throughout the visible regime with a pulse duration of 1 ps and a fluence of 10 nJ/mm². Note that the pulse duration of 1 ps is much longer than the typical plasmon decay time of several fs, and therefore, the continuous wave excited field distributions and dissipation distributions simulated here are a good approximation of those obtained under true pulsed illumination. The resulting temperature evolution for each of the structures is determined by numerically solving the heat-diffusion equation

$$\rho c_p \frac{\partial T}{\partial t} = Q + k \nabla^2 T, \quad (1)$$

where T is the time-dependent temperature distribution, Q is the power dissipation density, and ρ , c_p , and k are position

dependent density, specific heat capacity, and thermal conductivity, respectively, all obtained from literature and assumed to be temperature independent for the pulse energies used. The energy deposition in the nanoparticles follows from the simulated electric field distributions such as those shown in Figs. 1(b)–1(d), leading to inhomogeneous dissipation distributions. However, during the electron-phonon equilibration process, the locally generated hot electrons can move out of the excitation volume ballistically, resulting in a redistribution of the dissipated energy over distances exceeding 100 nm before equilibration with the lattice occurs for both silver and gold.^{25,26} Therefore, the particles are assumed to be heated with a total power determined by the simulated electric fields, distributed homogeneously throughout the particle corresponding to the relation $Q = \frac{1}{V} \int_V \frac{1}{2} \omega \varepsilon'' |\mathbf{E}(\mathbf{r})|^2 dV$ with V the particle volume, ω the angular frequency, $\mathbf{E}(\mathbf{r})$ the frequency dependent electric field distribution, and ε'' the imaginary part of the permittivity of the particle. The resultant temperature within each nanoparticle is approximately homogeneous (not shown), as expected based on the homogeneous deposited heat as well as the high thermal conductivity of silver and gold compared to that of water.

Figure 2 shows the volume-averaged temperature evolution $\Delta T(t)$ relative to the background temperature, at the three wavelengths corresponding to the modes in Figs. 1(b)–1(c). For the isolated Au nanoparticle excited at 530 nm (red line), the maximum ΔT is 0.23 K immediately after the laser pulse ($t = 1$ ps). The evolution of the temperature in the gold nanoparticle after the pulse is well described by a stretched exponential function²⁷ with a temperature relaxation time of $\tau = 16$ ps. This extremely rapid relaxation time is due in part to the large surface-to-volume ratio of the particle,¹⁶ enabling rapid heat transfer to the surrounding water.

The temperature evolution inside the particles in the silver dimer structure under excitation at 600 nm (blue line) shows a relatively small maximum temperature change of 0.08 K immediately after the laser pulse. The thermal relaxation time in this case is found to be 0.32 ns, 20 times larger

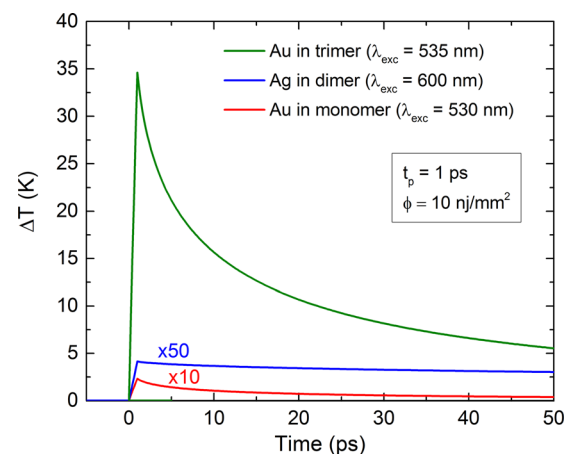


FIG. 2. Volume averaged nanoparticle temperature evolution under pulsed laser illumination with a fluence of 10 nJ/mm² and a pulse duration of 1 ps for a 10 nm diameter gold nanoparticle irradiated at 530 nm (red line), for a 80 nm silver nanosphere in a dimer structure with a gap of 5 nm irradiated at 600 nm (blue line) and for a gold nanosphere in a heterogeneous trimer structure composed of a 10 nm diameter gold nanoparticle between two 80 nm silver nanospheres irradiated at 535 nm (green line).

than observed for the isolated gold nanoparticle. Finally, the temperature evolution inside the 10 nm gold nanosphere in the heterogeneous trimer structure excited at 535 nm (green line) shows a large maximum temperature rise of 35 K immediately after the laser pulse with a rapid relaxation time of 16 ps. These results demonstrate the combined benefits of the cascaded trimer structure for use as a thermal nonlinear optical element: the large field enhancements enable large temperature changes, the gap between the central particle and the silver dimer prevents heat transfer to the cooler silver particles, and the strong field concentration enables extremely short thermal relaxation times.

To evaluate the thermo-optic response of these structures under pulsed excitation, we determine the change in optical properties achieved immediately after the excitation pulse, i.e., at the maximum achieved temperature. The temperature change for each excitation wavelength is converted to a change in the dielectric function of the particles using literature data for the thermo-optical coefficients of gold²⁸ and silver.²⁹ Finally, the absorption cross-section of the structures is calculated at each choice of illumination wavelength using the thermally modified dielectric functions, which enables the determination of the wavelength-dependent change in the absorption cross-section $\Delta\sigma_{\text{abs}}$. Finally, the nonlinear optical absorption performance of an aqueous suspension of these structures is described in terms of a figure of merit (FOM) given by

$$FOM \left(\frac{\text{m}^2}{\text{J}} \right) = \frac{\Delta\sigma}{\sigma\phi}, \quad (2)$$

where ϕ (J/m^2) is the fluence of the laser pulse and σ corresponds to the absorption cross-section spectra shown in Fig. 1. This parameter is large when a large relative change in the absorption cross-section can be achieved at low fluence, and mathematically corresponds to the inverse of the fluence required to obtain a thermally induced nonlinear absorption equal to the linear absorption at the assumed pulse duration of 1 ps. Note that these FOM calculations assume that the excitation field is aligned along the dimer or trimer axis.

Figure 3 shows the obtained FOM spectra for thermally induced nonlinear absorption in the silver dimer, the gold monomer, and the heterogeneous trimer discussed thus far, as well as for four additional trimers with varying Au nanoparticle diameters at the same edge-to-edge spacing. The FOM for isolated 10 nm gold nanospheres (purple line) shows saturable absorption (negative FOM) and reverse saturable absorption (positive FOM) below and above the dipolar plasmon resonance wavelength of the isolated gold nanoparticle, respectively. The largest FOM for this structure is $0.041 \text{ mm}^2/\mu\text{J}$, occurring at a wavelength of 555 nm. The FOM spectrum for the silver dimer structure (gray line) shows saturable absorption at energies above the plasmon resonance at 420 nm and below the plasmon resonance at 600 nm, and reverse saturable absorption between these two resonances with a maximum value of $0.01 \text{ mm}^2/\mu\text{J}$ at a wavelength of 560 nm. The FOM spectrum for the heterogeneous trimer structure (blue line) shows a shape similar to that of the isolated gold nanoparticle. However, the peak FOM achieved for the multi-material trimer structure is $1.78 \text{ mm}^2/\mu\text{J}$

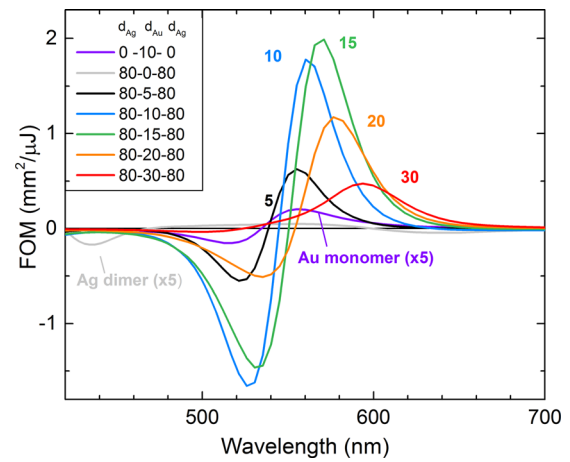


FIG. 3. Figure of merit for thermally induced nonlinear optical absorption of a 10 nm gold monomer, an 80 nm diameter silver dimer, and five heterogeneous trimer structures composed of two 80 nm diameter silver particles and central gold nanoparticles with diameters of 5, 10, 15, 20, and 30 nm and an edge-to-edge spacing of 5 nm after a 1 ps laser pulse.

μJ , a factor of 40 larger than that of the isolated gold nanoparticle. Based on the preceding discussion of the thermal simulations, this dramatic enhancement can be understood as the result of the strong field enhancement and the associated large energy dissipation inside the gold nanoparticle due to the cascaded plasmon resonance, enabling large changes of the gold refractive index.

Additional FOM spectra for nonlinear optical absorption were calculated for trimers with Au nanoparticle diameters of 5, 15, 20, and 30 nm while maintaining a 5 nm edge-to-edge spacing between all particles. The spectra all show similar features, with a maximum FOM of $2 \text{ mm}^2/\mu\text{J}$ observed for the trimer with a gold nanoparticle diameter of 15 nm. The existence of an optimum particle size that maximizes the nonlinear optical absorption performance can be explained by considering two factors that play a significant role in determining the thermally induced nonlinear optical response. The first factor is the temperature change which is strongly dependent on the gold related fractional absorption per unit volume.¹⁹ Decreasing the gold nanoparticle size increases the field enhancement factors that can be achieved by cascaded field enhancement.²⁴ This increases the absorption per unit volume of the gold particle and with it, the temperature change and the modification in its dielectric function. Counteracting this increase in the thermo-optic response of the gold particle is the volume dependent contribution of the gold nanoparticle to the total absorption cross-section. As the gold particle volume is reduced, its contribution to the total absorption cross-section of the trimer reduces. Consequently, large optically induced changes in its dielectric properties will only weakly affect the total absorption spectrum, resulting in a vanishing FOM for small nanoparticle sizes. The optimum gold particle size for large thermal nonlinear optical absorption thus occurs for a particle size that is small enough to enable a strong field enhancement and a large temperature change, while being big enough to significantly affect the total absorption coefficient. As a result of these effects, the thermally induced nonlinear optical absorption performance of a silver dimer structure (gray line) at 560 nm can be

enhanced by more than two orders of magnitude through the addition of only a single 10 nm diameter gold particle, corresponding to an added metal volume fraction of 0.1 vol. %. This remarkable enhancement demonstrates the application potential of heterogeneous plasmonic oligomers. The concepts presented here may be extended to clusters containing multiple particle shapes, sizes, and compositions, and may find applications in a wide range of fields where field enhancement, field concentration, or localized heat generation are needed.

In summary, we have investigated the thermally induced nonlinear optical response of plasmon resonant gold monomers, silver dimers, and heterogeneous trimers using full-field electromagnetic and transient thermal simulations. The attainable temperature changes and the associated thermally induced nonlinear optical response could be enhanced by utilizing cascaded field enhancement, resulting in an increase of the figure of merit for thermo-optically induced absorption of a heterogeneous trimer by a factor 40 relative to that of isolated gold nanoparticles. Response times smaller than a nanosecond and temperature changes as high as 35 K at a fluence as small as 10 nJ/mm² were predicted, making these structures of great interest for nonlinear optical absorption and low-power photothermal applications.

The authors would like to acknowledge Mr. Mahmood Mohagheghi from the Department of Mechanical and Aerospace Engineering at the University of Central Florida for valuable discussions regarding thermal simulation.

¹E. Lukianova-Hleb, Y. Hu, L. Latterini, L. Tarpani, S. Lee, R. A. Drezek, J. H. Hafner, and D. O. Lapotko, *ACS Nano* **4**, 2109 (2010).

²D. Lapotko, *Opt. Express* **17**, 2538 (2009).

³A. Vogel, N. Linz, S. Freidank, and G. Paltauf, *Phys. Rev. Lett.* **100**, 038102 (2008).

⁴F. Garwe, U. Bauerschafer, A. Csaki, A. Steinbruck, K. Ritter, A. Bochmann, J. Bergmann, A. Weise, D. Akimov, G. Maubach, K. Konig,

G. Huttmann, W. Paa, J. Popp, and W. Fritzsche, *Nanotechnology* **19**, 055207 (2008).

⁵C. M. Pitsillides, E. K. Joe, X. B. Wei, R. R. Anderson, and C. P. Lin, *Biophys. J.* **84**, 4023 (2003).

⁶P. Christopher, H. L. Xin, and S. Linic, *Nat. Chem.* **3**, 467 (2011).

⁷J. R. Adleman, D. A. Boyd, D. G. Goodwin, and D. Psaltis, *Nano Lett.* **9**, 4417 (2009).

⁸S. Mallidi, T. Larson, J. Aaron, K. Sokolov, and S. Emelianov, *Opt. Express* **15**, 6583 (2007).

⁹E. C. Garnett, W. S. Cai, J. J. Cha, F. Mahmood, S. T. Connor, M. G. Christoforo, Y. Cui, M. D. McGehee, and M. L. Brongersma, *Nat. Mater.* **11**, 241 (2012).

¹⁰L. Liu, P. Peng, A. M. Hu, G. S. Zou, W. W. Duley, and Y. N. Zhou, *Appl. Phys. Lett.* **102**, 073107 (2013).

¹¹J. C. Weeber, T. Bernardin, M. G. Nielsen, K. Hassan, S. Kaya, J. Fatome, C. Finot, A. Dereux, and N. Pleros, *Opt. Express* **21**, 27291 (2013).

¹²S. Kaya, J. C. Weeber, F. Zacharatos, K. Hassan, T. Bernardin, B. Cluzel, J. Fatome, and C. Finot, *Opt. Express* **21**, 22269 (2013).

¹³N. Rotenberg, A. D. Bristow, M. Pfeiffer, M. Betz, and H. M. van Driel, *Phys. Rev. B* **75**, 155426 (2007).

¹⁴G. Baffou, R. Quidant, and C. Girard, *Appl. Phys. Lett.* **94**, 153109 (2009).

¹⁵G. Baffou, C. Girard, and R. Quidant, *Phys. Rev. Lett.* **104**, 136805 (2010).

¹⁶G. Baffou, R. Quidant, and F. J. G. de Abajo, *ACS Nano* **4**, 709 (2010).

¹⁷C. L. Baldwin, N. W. Bigelow, and D. J. Masiello, *J. Phys. Chem. Lett.* **5**, 1347 (2014).

¹⁸A. O. Govorov, W. Zhang, T. Skeini, H. Richardson, J. Lee, and N. A. Kotov, *Nanoscale Res. Lett.* **1**, 84 (2006).

¹⁹S. Toroghi and P. G. Kik, *Phys. Rev. B* **90**, 205414 (2014).

²⁰Microwave Studio, Computer Simulation Technology, Darmstadt, Germany, 2013.

²¹Multiphysics Studio, Computer Simulation Technology, Darmstadt, Germany, 2013.

²²E. D. Palik, *Handbook of Optical Constants of Solids* (Academic Press, New York, 1985).

²³P. B. Johnson and R. W. Christy, *Phys. Rev. B* **6**, 4370 (1972).

²⁴S. Toroghi and P. G. Kik, *Appl. Phys. Lett.* **100**, 183105 (2012).

²⁵J. Hohlfeld, J. G. Muller, S. S. Wellershoff, and E. Matthias, *Appl. Phys. B* **65**, 681 (1997).

²⁶J. Hohlfeld, S. S. Wellershoff, J. Gudde, U. Conrad, V. Jahnke, and E. Matthias, *Chem. Phys.* **251**, 237 (2000).

²⁷M. Hu and G. V. Hartland, *J. Phys. Chem. B* **106**, 7029 (2002).

²⁸M. Rashidi-Huyeh and B. Palpant, *Phys. Rev. B* **74**, 075405 (2006).

²⁹S. T. Sundari, S. Chandra, and A. K. Tyagi, *J. Appl. Phys.* **114**, 033515 (2013).